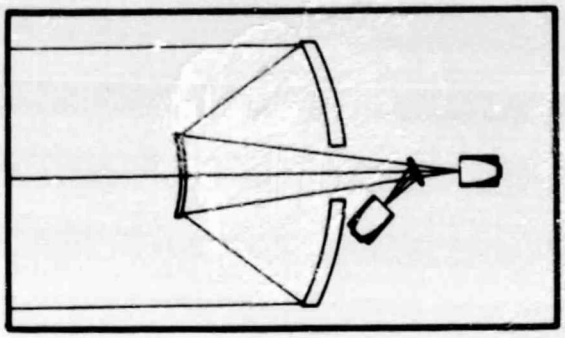

SPECTROPHOTOVOLTAIC ORBITAL POWER GENERATION

Gary Knowles
Dave Stoltzman
Ray Lin
Sau Kwan Lo

CONTRACT NO. NAS 8-33511
MID-TERM REPORT

DECEMBER 18, 1980

Prepared for

GEORGE C. MARSHALL SPACE FLIGHT CENTER
HUNTSVILLE, ALABAMA

By

Honeywell
SYSTEMS & RESEARCH CENTER
2600 RIDGWAY PARKWAY
MINNEAPOLIS, MINNESOTA 55413

(NASA-CR-161795) SPECTROPHOTOVOLTAIC ORBITAL POWER GENERATION Progress Report (Honeywell Systems and Research) 59 p
HC A04/MF A01 CSCL 10A

N81-25508

Unclas
G3/44 27866

TABLE OF CONTENTS

LIST OF FIGURES

LIST OF TABLES

1.0 INTRODUCTION AND SUMMARY

1.1 Summary of Phase I

During the previous phase of the program, a spectral splitting photovoltaic concept was defined. In this concept, the energy spectrum is split into different bands in which photon energy is effectively converted into electrical energy via photovoltaic cells that have matching spectral response. The efficiency of the system also increases with concentration ratio if the temperature of the cell is maintained constantly $\sim$ 300K. Assuming this condition is met, a system with 1000 : 1 concentration ratio is defined, using a cassegrain telescope as the first stage concentration (270 x) and compound parabolic concentrators (CPC) for the second stage concentration of 4.7 x for each spectral band. Using reported state-of-the-art (S.O.A.) solar cells device parameters and considering structural losses due to optics and beamsplitters, the efficiencies of one-to-four-cell systems were calculated with efficiencies varying from $\sim$ 22% to $\sim$ 30%. Taking into account cost of the optics, beamsplitter, radiator, and the cost of developing new cells the most cost effective system is the GaAs/Si system.

The advantages of the spectrophotovoltaic concept are (1) the increase in photoelectric conversion efficiency without development of new materials and cells, (2) intrinsic particle radiation hardening since the cells are not directly exposed to particle radiation, and (3) intrinsic resistance to laser damage since the acceptance angle of the concentrator system is only $\pm$ 0.5^{o} pointing at the sun.

1.2 Program Objectives for Phase II

For this phase of the program the objective is to define and design a subscale model which will demonstrate the hardware feasibility of selected components of the full-scale spectrophotovoltaic orbital power generation system up to a concentration ratio of 1000 : 1. The design for ground-based testing

will be in sufficient detail to produce a subscale model capable of demonstrating the performance characteristics of the major components and the integrated system.

1.3 Highlights and Summary of Mid-Term Progress

The program is carried out under six major task areas. They are:

1. Model Definition
2. Optical Design
3. Beamsplitter Design
4. Thermal/Mechanical Design
5. Model Coating
6. Testing Plan

The first task is completed and the others are in progress.

The subscale model defined is a 10" aperture system with effective concentration ratio up to 1000 : 1 similar to that defined in Phase I. The partially concentrated solar spectrum will be divided into two bands by a beamsplitter then focused onto two selected cells.. The chosen cells are well developed GaAs and Si solar cells. Both reflective and transmitting mode to GaAs denoted by GaAs/Si and Si/GaAs respectively will be tested since each configuration has its own merits. The model to be built is aimed at demonstrating the high conversion efficiency due to both spectrum splitting and high concentration ratio of the defined concept. In addition thermal data on various system components will be taken which will shed light on system losses and thus lead to a more optimal design. The components of the system to withstand such high concentration will also be tested to ascertain the feasibility of such a concept.

The advantages of indoor testing under a solar simulator are the ability to simulate AMO spectrum and a more controllable test environment than outdoor testing. However the large divergence angle of the available simulator

for full sun intensity is not compatible with the optical design that was finalized in Phase I. The optical design that will accommodate $\pm$ 3.0° incoming beam has much higher secondary obscuration and much higher number of reflections inside the CPC's which would be required to handle most of the concentration. The resulting design is both inefficient and has little resemblance to the space system and therefore was abandoned.

The compromise position is to adjust the simulator so that the divergence angle is similar to that of the sun. This can be accomplished by decreasing the xenon source aperture. The penalty is in decreasing the simulator intensity i.e., indoor testing cannot be fully tested at full sen intensity. However, enhancement of conversion efficiency by spectrum splitting can still be demonstrated.

The optical design for the subscale model is therefore a scaled down version of the design in Phase I with an increase of the back focal length from 3" to 6" to allow room for thermal measurement of the CPC and solar cell closest to the primary. This affects the secondary obscuration which consequently increased from 7% to 10%. The design was verified by ray-tracing that over 95% of the spectral energy would be imaged onto the solar cells after one reflection at the CPC's. Three manufacturing methods for the optical components are explored. Among these electroforming, a version of electroplating, appears to be the most economical for the CPC's. Diamond tuning and conventional glass grinding appear best for the primary and secondary.

Two beamsplitter designs are completed utilizing a 65-layer Ta_2O_5/MgF_2 for the GaAs/Si configuration and a 21-layer CaF_2/ThO_2 for the Si/GaAs configuration. The second design has a reflection spike at 0.35 μm which would be undesirable if GaAs has significant spectral response below 0.4 μm.

Inquiries into the S.O.A. [1] spectral response of the solar cells (both GaAs and Si) indicate a very sharp cut-off between 0.4 to 0.5 μm. This is in contradiction to our calculation in Phase I. It is important that our design should be optimized for available S.O.A. solar cells and not ideal cells. Therefore immediate action is being taken to obtain more detailed information on the cells from potential suppliers.

Mechanical support for the system aimed at ground based laboratory and field testing has been detailed and is being finalized with technical drawings Design for thermal testing of the CPC's and cells is also completed. Due to the small amount of thermal dissipation in a subscale system, insulation around the measured components is required to obtain accurate data. If loss due to air convection can be neglected then a 5% error in the measurement is foreseen. Thermal analysis on the 10" system based on predicted cell performance shows ∿ 23% conversion efficiency (power output/total flux intercepted) for the GaAs/Si system and ∿ 21% for the Si/GaAs system.

Cost estimate for building and testing the subscale model is ∿ $210K.

---

(1) Private Communication, Dr. Brandhorst of NASA Lewis Research Center.

2.0 TECHNICAL PROGRESS

2.1 Model Definition

The purpose of designing and eventually constructing the subscale model is to demonstrate the enhanced power generation efficiency of the spectro-photovoltaic concept defined in Phase I, and to prove hardware feasibility of the optical components including the beamsplitter and the solar cells. The designed model, therefore, should be of close resemblance to the full-scale space system, such that the information obtained could be scaled up to the full system*.

Based on this criteria, drastic redesign of the optical system to make it suitable for full sun simulator testing was rejected. While the basic design is unchanged, the question of how large to make the subscale model remains. In selecting a aperture size the drawing considerations were to make the aperture large enough such that the amount of energy collected would be readily measureable, and to make the concentrator small enough to be reasonably priced and readily portable. Consideration was given to system with a primary diameter up to 16 inches. Construction methods considered were both conventional glass grinding and diamond turning of a metal mirror. Analysis of the energy conversion processes showed that for a 10 inch aperture system the thermal and electric output for each cell would be in the 0.1 to 6 watt range. Electric power can readily be measured to $\pm$ 100 micro watt accuracy and the thermal measurements can be made to approximately $\pm$ 5 milliwatt accuracy. A 16 inch aperture system would increase the thermal and electric signal output by 2.5 times that of a 10 inch system with only a small increase in measurement uncertainty.

---

*It is not clear at this point whether the full scale system would be a direct scale-up to $\sim$ 20 m aperture single system or a number of smaller systems with the same total effective aperture area for a power generation of 100 kW.

Fabrication of the primary mirror by diamond turning is currently limited to surfaces less than 14 inches in diameter. Convention glass grinding for a 16 inch f/0.7 mirror would be very expensive. A third fabrication technique considered was electroforming. This method could produce a very thin 0.20 inch thick mirror which would be very portable. For a single unit construction it would be a very expensive fabrication technique since a high quality master mold must be fabricated on which the metal can be plated. With these considerations in mind, the decision was made to limit the subscale model to the more economically constructed 10 inch aperture.

The model should be able to demonstrate qualitatively and quantitatively the enhancement of power conversion with a beamsplitter and with increasing concentration ratio as compared to an equivalent area planar array. Thus the model should be tested with and without the beamsplitter as well as at variable concentration ratios by reducing the source intensity or placing neutral density filters in front of the aperture, and comparing the result to a planar array of Si solar cells which have the same aperture area. By monitoring various components of the system prior to and after integration, information on system losses would be available to aid in optimizing future designs.

2.2 Solar Cells

There is no development of solar cells in this program. It is desirable to use the most developed cells for the subscale model for demonstration of the spectrophotovoltaic concept. The ideal size of the solar cells for the subscale model is 0.28" in diameter. All the companies we contacted are willing to custom make Si and/or GaAs cells at a cost of ~ $2000 to $5000. On the other hand if we can use the available larger size cells, it will be at minimal or no cost to the program. Since the dark current from the cell can either be measured or calculated, and is expected to be much smaller than the photogenerated current, cells of sizes larger than required by the model can be used. The information obtain from the potential suppliers is given in Table 1.

TABLE 1. CONCENTRATOR SOLAR CELLS

Type of Cell	GaAs	GaAlAs/GaAs	Si	Si
Manufacturer	Varian	Rockwell International Thousand Oaks, CA	Solarex Rockville, MD	Applied Solar Energy, City of Industry, CA
Cell Size	1/3" & 1/2" dia. circle	1 cm dia. circle or 0.25" square	2 1/4" dia. circle or 2 cm x 2 cm square	2 cm x 2 cm square
Highest Available Concentration	1700	1000	200	200
Efficiency (%)	23% (1000x)	22% (1000x)	> 10% (50x)	14-15% (200x)
Grid Coverage	< 5%	~ 10%	5-8% (square) 10% (circle)	7%
Mounting	Soldered to Aluminum		Adhesively bonded to Aluminum	Solderable Ti-Pd-Ag backplate
Notes	Intrinisic resistance 9×10^{-5} Ω/cm^2 will provide 1000x - 1700 x cells	Resistance $5\text{-}6 \times 10^{-3}$ Ω will custom make 1000x cells	Fill Factor 72% (200x) will custom make 1000x cells	Resistance 1.5×10^{-3} Ω will develop 500x - 1000x cells

It is not clear under what conditions the quoted efficiencies of the cells were measured and how they are defined. The GaAs is especially high compared to the S.O.A. performance (17% AMO) acknowledged by NASA Lewis Research Center. More detailed information e.g., spectral response of the cells needs to be obtained.

For the demonstration of the spectrophotovoltaic concept, a flat panel of Si solar cells with equivalent 10" diameter areas should be used for comparison.

2.3 Optical Design

2.3.1 Background

Power requirements for space missions are expected to be in the several kilowatts of electrical and thermal power for heating/cooling and direct electrical applications. When thermal power is required at high temperatures, concentration of solar energy seems to be a practical way to obtain the desired temperatures. And for directly converting solar flux to electricity, a concentration system allows the size of the solar cells to be reduced by the concentration ratio.

Earlier work indicated that the concentration system should be able to produce optical concentrations in the vicinity of 1000:1. To achieve this goal, a survey of collector-concentration concepts was conducted. A two-stage concentration system was found to be optimum, with each stage performing some of the concentration. The first stage was chosen to be a Cassegrain telescope because this type of optics would keep the collector close to the spacecraft. The second stage of concentration employs compound parabolic concentrators. A schematic of this system, for a three-cell configuration, is shown in Figure 1.

The first-stage concentration of the Cassegrain is the ratio of the area of the entering beam to the area of the image; the second-stage concentration of the CPC's is the ratio of the areas of the entrance and exit apertures, assuming the exit aperture is the same as the solar cell array. The resultant

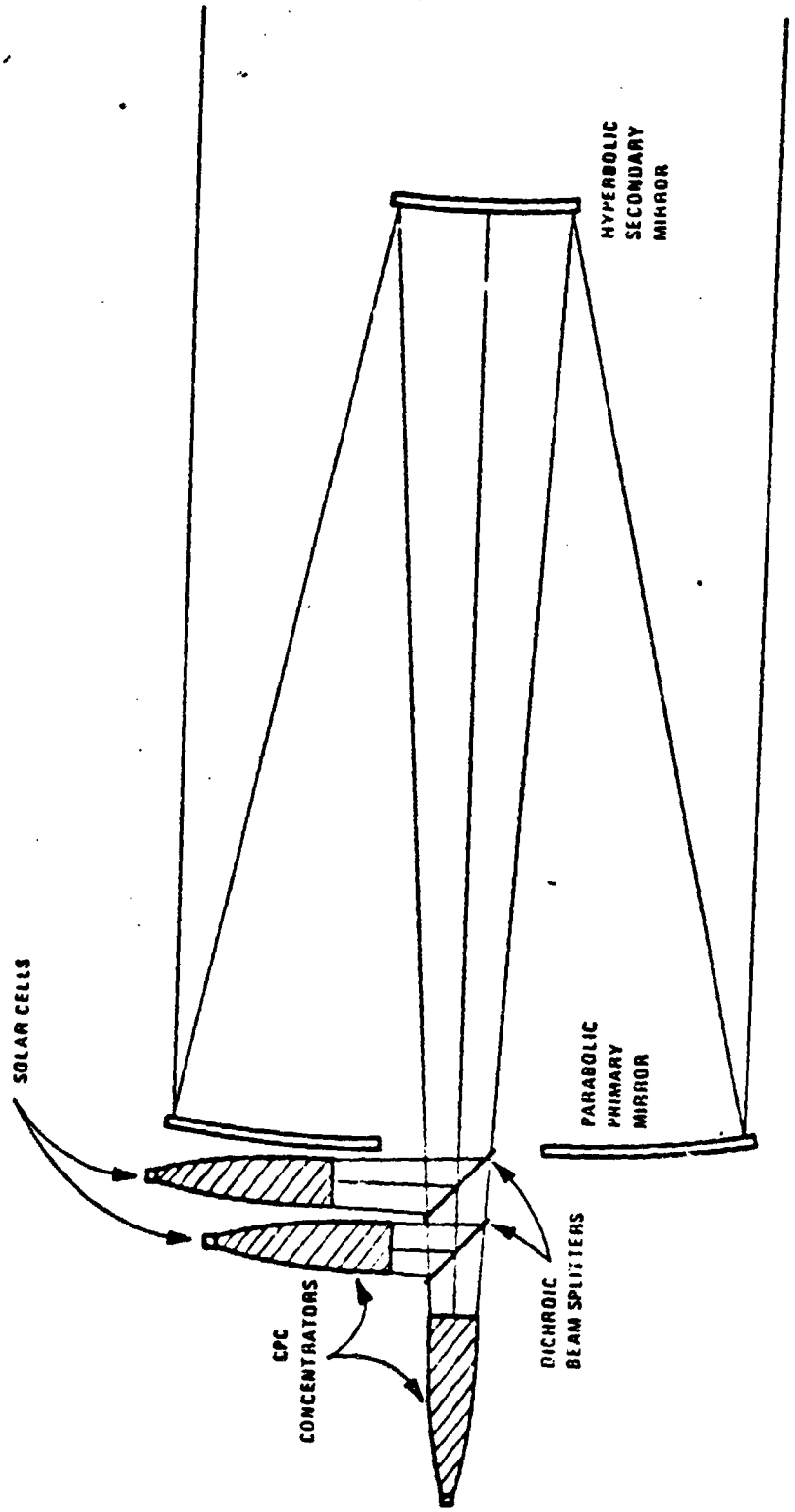

Figure 1. Schematic of Optical System

optical concentration of the system is the product of the concentration of the telescope and the CPC.

In order to determine the optimum concentration ratio for each stage, a preliminary system's design was performed on two systems with f-numbers of 2 and 5. These two systems are shown in Figures 2 and 3. Some general design considerations resulted from this comparison. In the f/2 system most of the concentration was performed by the Cassegrain, resulting in a very compact system. However, the components have steep curvatures, large concentrated power is incident on the beamsplitters, and a relatively large obscuration is present. In the f/5 system, most of the concentration is performed by the CPC's, resulting in a large system. The components are less steeply curved and less power is incident on the beamsplitters. While the obscuration is reduced in this latter configuration, the system becomes very large.

Since a large number of design parameters are involved in the actual design configuration, a computer program was written using parametric equations for all the design parameters. This program was used to optimize for the best system. An f/3.5 system having concentration ratios of 270 and 4.7 for the first and second stages respectively, was found to be optimum. A detailed design of this system was then performed, including a complete ray trace of the optical components. A schematic of the system is shown in Figure 4. The optical description of this system scaled to a primary diameter of 1.0 is shown in Figure 5. The system design parameters are detailed in Figure 6.

f/1.0 Primary Mirror
2.0x Secondary Mirror
System EFL = 35.6 m; f/2.0
Secondary Obscuration = 15%

CPC Diameter = 0.62 m
CPC Length = 0.37
CPC Concentration Ratio = 1.425

BS_1 Major Axis = 1.4 m
BS_2 Major Axis = 2.2 m

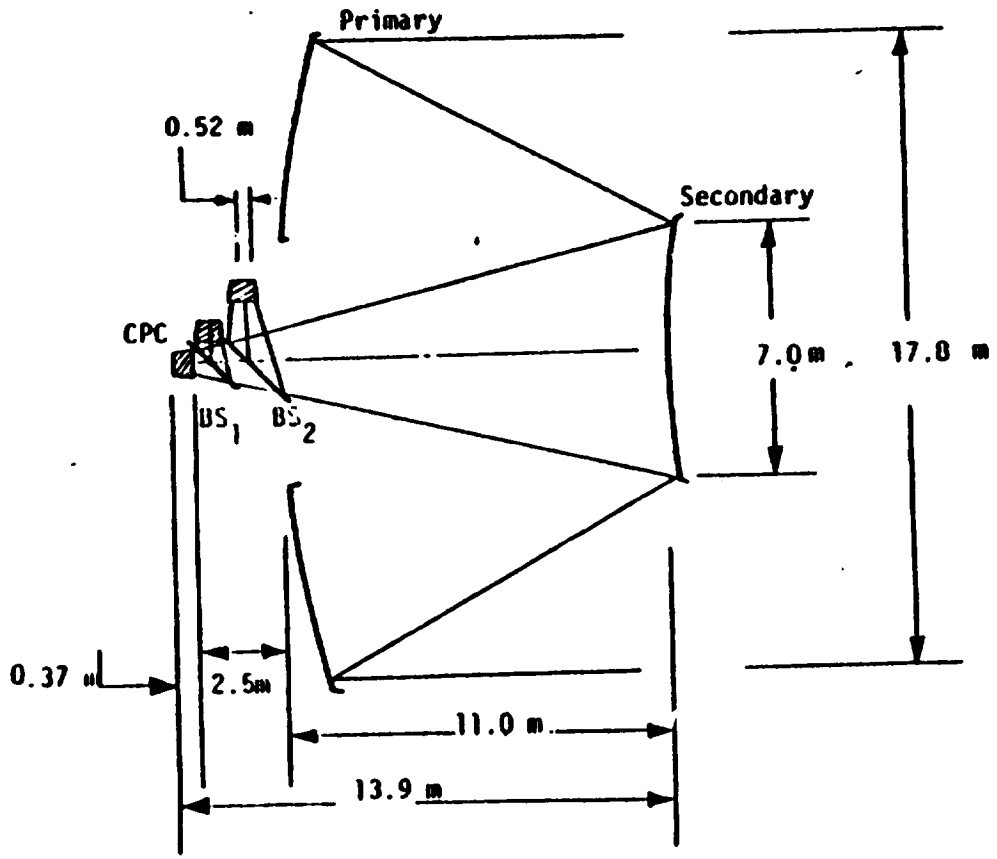

Figure 2. 100 kW f/2.0 Optical System

f/2.0 Primary Mirror
2.5x Secondary Mirror
System EFL = 89.0 m; f/5.0
Secondary Obscuration = 10%

CPC Diameter = 1.55 m
CPC Length = 2.90 m
CPC Concentration Ratio = 8.91

BS_1 major axis = 2.2 m
BS_2 major axis = 2.8 m

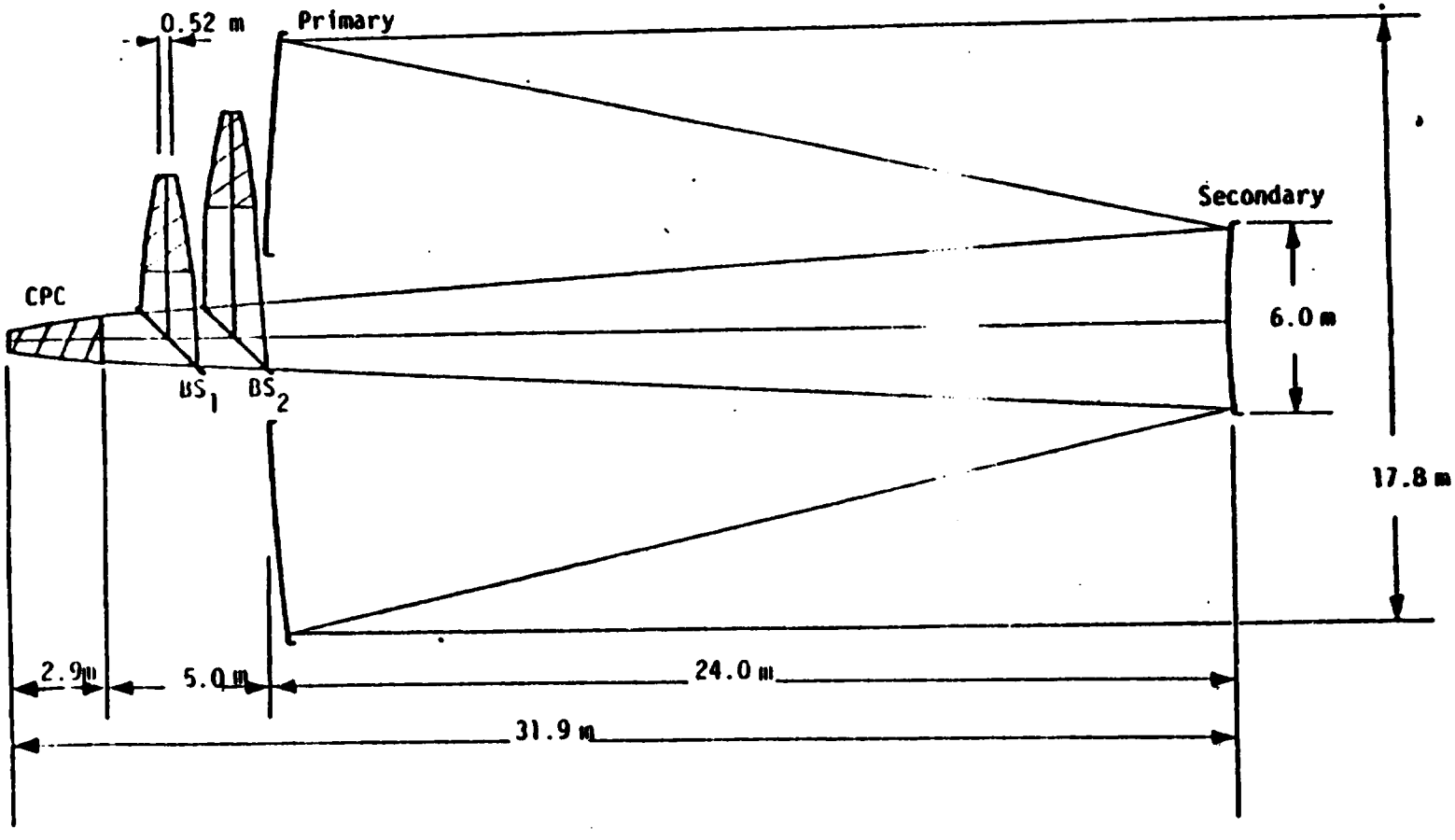

Figure 3. 100 kW f/5.0 Optical System

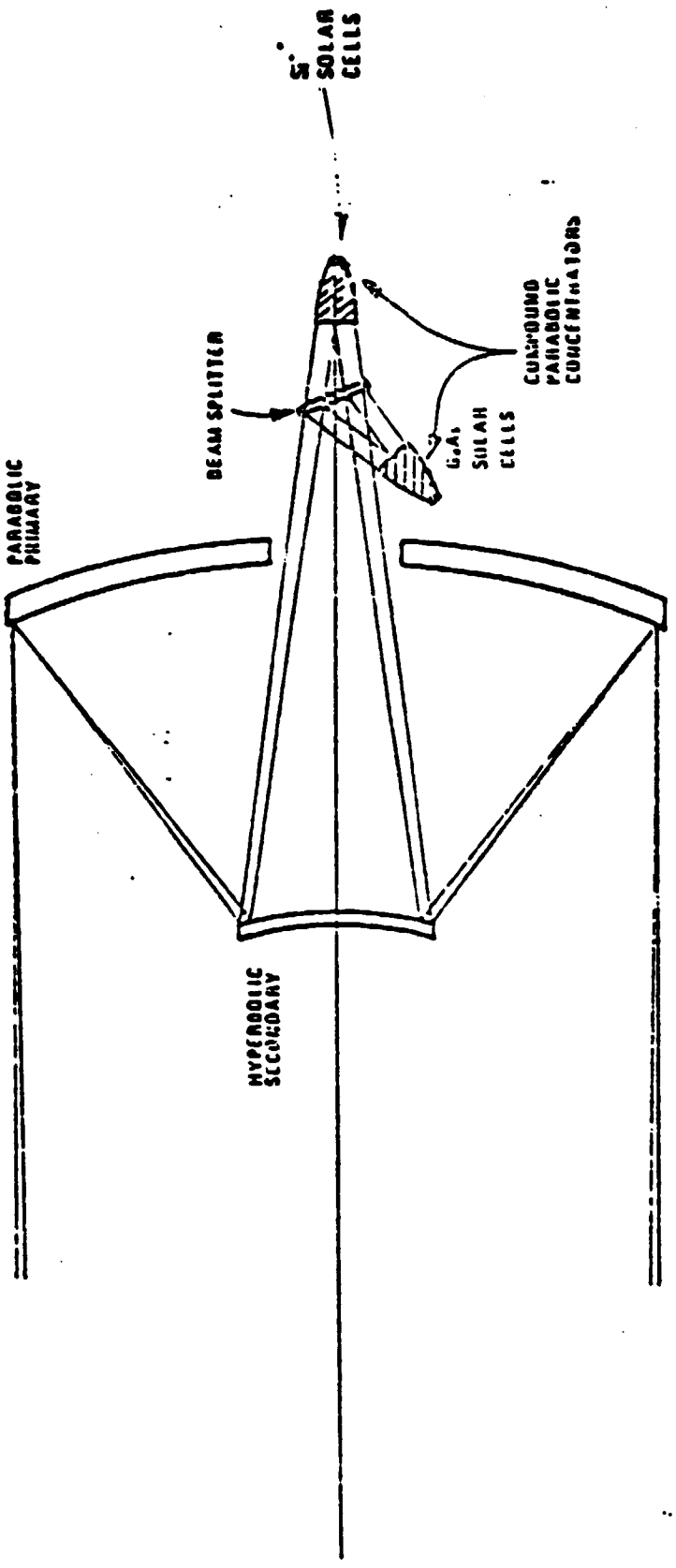

Figure 4. Optical/Mechanical System Layout

****

SOLAR CONCENTRATOR - FINAL DESIGN
SYSTEM SCALED TO PRIMARY DIAMETER = 1
CPC REPRESENTED AS ELLIPSE

****

LENS UNITS ARE INCHES

REF OBJ HT		REF AP HT	OBJ SURF	REF SURF	IMG SURF
-.436335E+08	(.25 DG)	.50000	0	1	17

EFL	BF	F/NBR	LENGTH	GIH
3.5000	0.0000	3.50	.4532	.0165

WAVL NBR	1	2	3	4	5
WAVELENGTH	.58756	.48613	.65627	.43584	.70652
SPECTRAL WT	1.0000	1.0000	1.0000	1.0000	1.0000

BASIC LENS DATA

SURF	CV	RD	TH	MEDIUM
0	0.000000	0.000000	1.000000E+10	AIR
1	-.714286	-1.400000	-.522000	REFL
2	-2.247191	-.445000	.490000	REFL
3	0.000000	0.000000	.085244	AIR
4	0.000000	0.000000	.010942	AIR
5	-103.737668	-.009640	-.010942	REFL
6	0.000000	0.000000	.010942	AIR
7	-103.737668	-.009640	-.010942	REFL
8	0.000000	0.000000	.010942	AIR
9	-103.737668	-.009640	-.010942	REFL
10	0.000000	0.000000	.010942	AIR
11	-103.737668	-.009640	-.010942	REFL
12	0.000000	0.000000	.010942	AIR
13	-103.737668	-.009640	-.010942	REFL
14	0.000000	0.000000	.010942	AIR
15	-103.737668	-.009640	-.010942	REFL
16	0.000000	0.000000	0.000000	AIR
17	0.000000	0.000000	0.000000	AIR

CC AND ASPHERIC DATA

SURF	CC
1	-1.000000E+00
2	-2.250000E+00
5	-9.911A0E-01
7	-9.911A0E-01
9	-9.911A0E-01
11	-9.911A0E-01
13	-9.911A0E-01
15	-9.911A0E-01

Figure 5. Optical Layout for Solar Concentrator

Parameter	Parameter Value	
	Normalized System	GaAs|Si, 100 kW
Primary diameter	1m	20.43m
Primary focal length	0.7m	14.30m
Primary conic constant	-1	-1
Secondary diameter	0.26m	5.31m
Secondary focal length	0.2225m	4.55m
Secondary conic constant	-2.25	-2.25
Secondary Magnification	5.0	5.0
Obscuration (Area)	7.3%	7.3%
Obscuration efficiency	0.927	0.927
CPC diameter	0.061m	1.25m
CPC length	0.085m	1.74m
Cassegrain concentration	269.63	269.63
CPC concentration	4.66	4.66
System concentration (Design)	1256.60	1256.60
System focal length	3.5m	71.51m
System f-number	3.5	3.5
Beam splitter area	$0.0075m^2$	$3.13m^2$
Solar cell array diameter	0.0282m	0.576m

Figure 6. Solar Concentrator Final Design

2.3.2 Current Phase II Status

Having designed an optimum solar concentration system in the previous phase, the final optical system design (Figure 4) could then be scaled down to an appropriate size for field testing as a demonstration model. The actual size of the model would depend on the available sizes of the solar cells, and the concentration ratio to be demonstrated. In addition, considerations of the testing environment (ambient sunlight vs. laboratory solar simulator) needed to be considered regarding the final scale of the model.

Thus, an initial comparison was made between two systems of 10" and 16" aperture, scaled from the final design of the previous phase. The parameter values for these two systems are given in Figure 7. Both of these systems require CPC's whose size is reasonable to fabricate, but the fabrication of the 16" primary mirror appeared to be questionable. At present, diamond machining lathes cannot handle a 16" diameter, while a glass mirror which is ground and polished conventionally would be extremely expensive and heavy in this large size.

Concurrently with the discussions on the size requirements of the subscale model, the possibility of using a laboratory solar simulator was researched. The simulators could produce beam apertures from 5" to 10", although some modification of the simulator optical system would be required to produce a 10" aperture. Model designs for these apertures were investigated, and the pertinent design parameters for representative 5" and 10" systems are given

Parameter	Parameter Value		
	Normalized System	10" Primary	16" Primary
Primary diameter	1	10.0 in	16.0 in
Primary focal length	0.7	7.0 in	11.2 in
Primary conic constant	-1	-1	-1
Secondary diameter	0.26	2.6 in	4.16 in
Secondary focal length	0.2225	2.225 in	3.56 in
Secondary conic constant	-2.25	-2.25	-2.25
Secondary Magnification	5.0	5.0	5.0
Obscuration (Area)	7.3%	7.3%	7.3%
Obscuration efficiency	0.927	0.927	0.927
CPC diameter	0.061	0.61 in	0.98 in
CPC length	0.085	0.85 in	1.36 in
Cassegrain concentration	269.63	269.63	269.63
CPC concentration	4.66	4.66	4.66
System concentration (Design)	1256.60	1256.60	1256.60
System focal length	3.5	35.0 in	56.0 in
System f-number	3.5	3.5	3.5
Beam splitter area	0.0075	0.75 in^2	1.92 in^2
Solar cell array diameter	0.0282	0.282 in	0.451 in

Figure 7. Solar Concentrator Scaled Designs

in Figure 8. The substantial increase in the source divergence angle for the laboratory simulators was found to place severe demands on the CPC's. Most of the concentration was now being performed by the CPC's instead of the Cassegrain, which resulted in very long CPC's, and much more obscuration by the secondary mirror.

Thus, considerations of the manufacturability and efficiency of the CPC's for systems designed for large source divergence, lead us to conclude that such designs are not desirable. The solar simulator can be modified to aperture down the source, which decreases the angular divergence, but this also reduces the intensity significantly. It is felt, however, that adequate intensity will still be had, to allow accurate concentration measurements. The system was therefore designed to have a 10" aperture, concentrating a $\pm 0.5^{o}$ or smaller source. The design parameters for this system are listed in Figure 9, and a schematic drawing is given in Figure 10. The optical raytrace computer listing is given in Figure 11.

Essentially, the only change needed in this system, from the scaled system of the last phase, is to scale it to 10" aperture and increase the back focus slightly to allow sufficient clearance for thermal measurements and mechanical mounting of the CPC's. This results in a slightly larger secondary placed slightly closer to the primary, and a 3% increase in the system obscuration.

Primary Diameter =	5.0"	10.0"	10.0"
Primary Focal Length =	3.5"	7.0"	7.0"
Primary F/# =	0.7	0.7	0.7
Secondary Magnification =	5.0	5.0	5.0
System Back Focal Length =	4.0	4.0	3.0
Source Angular Subtense =	$\pm$ 3.0^0	$\pm$ 1.5^0	$\pm$ 0.5^0
System Focal Length =	17.50"	35.00"	35.00"
System F/# =	3.50	3.50	3.50
Secondary Focal Length =	-1.56"	-2.29"	-2.23"
Secondary Diameter =	1.81"	2.89"	2.60"
Primary-Secondary Separation =	2.25"	5.17"	5.33"
Secondary Obscuration =	0.16"	0.08"	0.07"
Obscuration Efficiency =	0.84"	0.92"	0.93"
CPC Entrance Aperture Dia. =	1.83"	1.83"	0.61"
Concentration of Cassegrain =	7.43	29.76	269.63
Solar Cell Diam. =	0.16"	0.31"	0.28"
Concentration of CPL =	134.74	33.65	4.66
Length of CPC =	11.57"	6.23"	0.85"
System Concentration =	1000	1000	1256

Figure 8. System Design Parameters for Different Divergence Sources

Primary Diameter =	10.0"
Primary Focal Length =	7.0"
Primary F/# =	0.70
Secondary Magnification =	5.0
System Back Focal Length =	6.0"
Source Angular Subtense =	$\pm$ 0.5^{o}
System Focal Length =	35.00"
System F/# =	3.50
Secondary Focal Length =	-2.71"
Secondary Diameter =	3.18"
Primary-Secondary Separation =	4.83"
Secondary Obscuration =	0.10
Obscuration Efficiency =	0.90
CPC Entrance Aperture Dia. =	0.61"
Concentration of Cassegrain =	269.63
Solar Cell Diameter =	0.28"
Concentration of CPC =	4.66
Length of CPC =	0.85"
System Concentration =	1256

Figure 9. System Design Parameter for Subscale Model

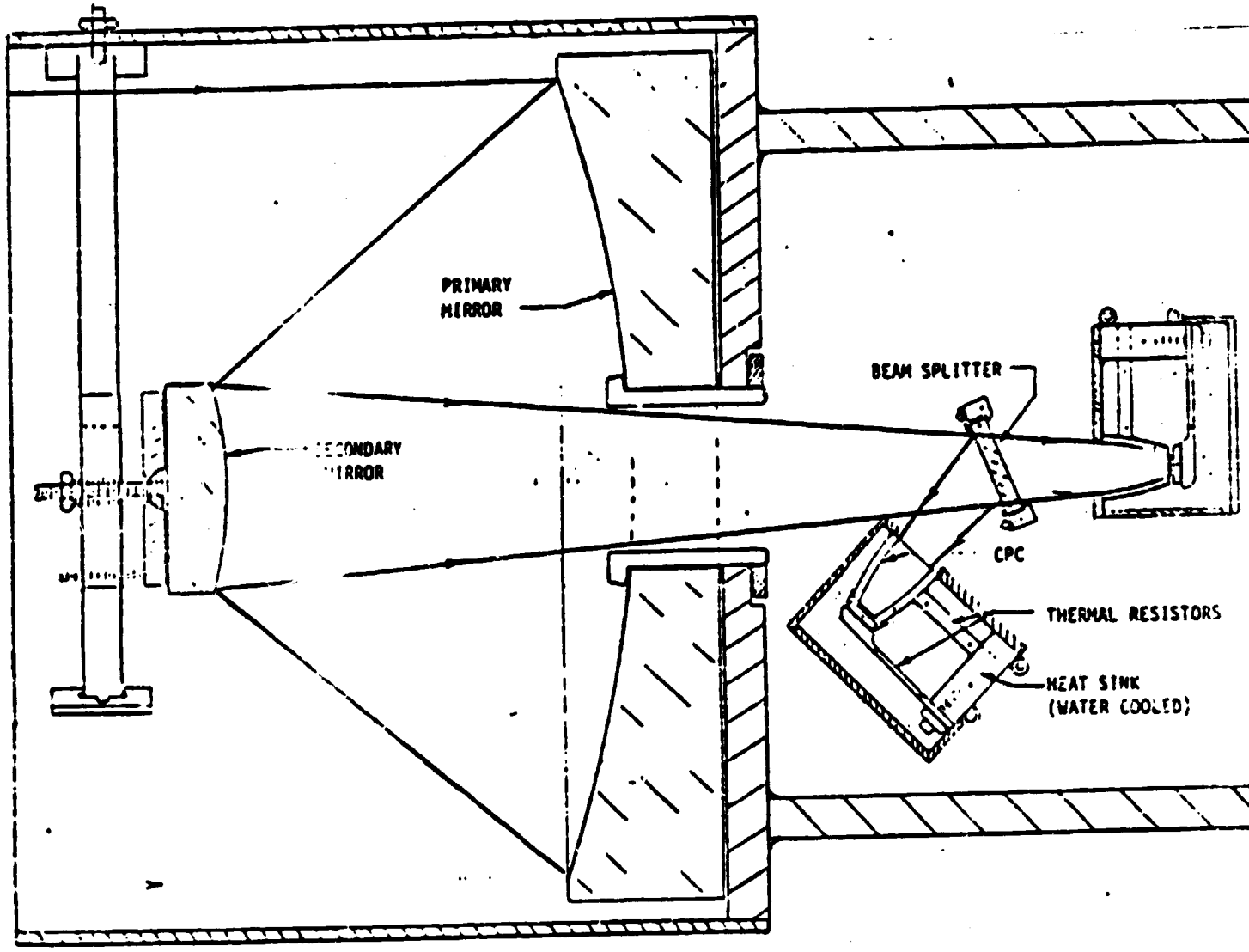

Figure 10. Subscale Model Design

****

SOLAR CONCENTRATOR - MOD1
PRIMARY DIAM=10, BF=6(GRN)
ALPHA=2

****

LENS UNITS ARE INCHES

REF OBJ HT		REF AP HT	OBJ SURF	REF SURF	IMG SURF
-.436335E+08	(.25 DG)	5.00000	0	1	11

EFL	BF	F/NBR	LENGTH	GIH
1.8464	0.0000	.18	6.8524	-.2075

WAVL NBR	1	2	3	4	5
WAVELENGTH	.58756	.48613	.65627	.43584	.70652
SPECTRAL WT	1.0000	1.0000	1.0000	1.0000	1.0000

BASIC LENS DATA

SURF	CV	RD	TH	MEDIUM	RN
0	0.000000	0.000000	1.000000E+10	AIR	
1	-.071429	-14.000000	-4.833333	REFL	
2	-.184615	-5.416667	10.833333	REFL	
3	0.000000	0.000000	.852440	AIR	
4	0.000000	0.000000	.109420	AIR	
5	-10.373767	-.096397	-.109420	REFL	
6	0.000000	0.000000	.109420	AIR	
7	-10.373767	-.096397	-.109420	REFL	
8	0.000000	0.000000	.109420	AIR	
9	-10.373767	-.096397	-.109420	REFL	
10	0.000000	0.000000	0.000000	AIR	
11	0.000000	0.000000	0.000000	AIR	

CC AND ASPHERIC DATA

SURF	CC	AD	AE	AF	AG
1	-1.000000E+00				
2	-2.250000E+00				
5	-8.997805E-01				
7	-8.997805E-01				
9	-8.997805E-01				

Figure 11. Raytrace Listing of the 10" Subscale Model

2.3.3 Future Optical Considerations in Phase II

Having designed the components of the optical concentration system, some details of the components relating to their manufacture remain to be specified. In the previous phase, we investigated the tolerance sensitivity of the Cassegrain mirrors, and found the secondary to be less sensitive to surface fabrication errors than the primary. This analysis will be continued to define specific surface shape tolerances for the Cassegrain as well as the CPC's. The tolerancing will provide an envelope for the surface shape profiles of the components, to aid in their manufacture.

The tolerance analysis will also address the alignment of the components in the system. The concentration of each element and its allowable angular tilt from the optical axis will be analyzed, to insure adequate performance for the system. In addition, the system's angular sensitivity to source misalignment will be analyzed, since both a laboratory source and the sun will likely be concentrated. This will also give a first-order indication of the expected tracking requirements for an orbital concentrator, as well as the necessary tracking accuracy for the field testing of the model.

We also plan to investigate other areas relating to the optical components. We nominally specified that the reflectivity of the 3 mirror surfaces in the system (primary, secondary, CPC) would be 95%, resulting in an optical efficiency of 85%. We are investigating higher efficiency coatings to hopefully bring the reflectivity to 98% or higher, which would boost the efficiency of 3 surfaces to 94%.

The fabrication methods for the individual components for the 10" model will be researched further, to define the best method to use (diamond machining, conventional grinding and polishing, electroforming, etc.). This effort will interface closely with the rest of the mechanical design of the model, to insure an optimum model configuration for laboratory and field testing.

An additional consideration during this phase, is a preliminary analysis of our in-house solar simulators. The optical configuration of these devices will be measured, to aid in any redesign efforts which might be required. We anticipate having to aperture down the source to decrease the output beam divergence, as well as probably having to increase the output beam diameter to 10".

The concept of using tandem solar cells appears to be of some merit once again, since the model will employ only one beamsplitter in a two-cell configuration. While a transmission tandem cell configuration is unavailable at the current time and would present non-negligible losses from grid structures on the surfaces, the possibility of performing some testing of tandem cells in a reflection mode appears feasible. A schematic of the configuration for a two-cell reflection mode is shown in Figure 12. Basically a highly reflecting coating is applied to the backside of a Si cell directly. This results in a larger Si solar cell, with less concentration. The tradeoff to be made is the cost of this larger Si cell with its multilayer coating, versus the cost of the beamsplitter plus another CPC and a smaller Si cell.

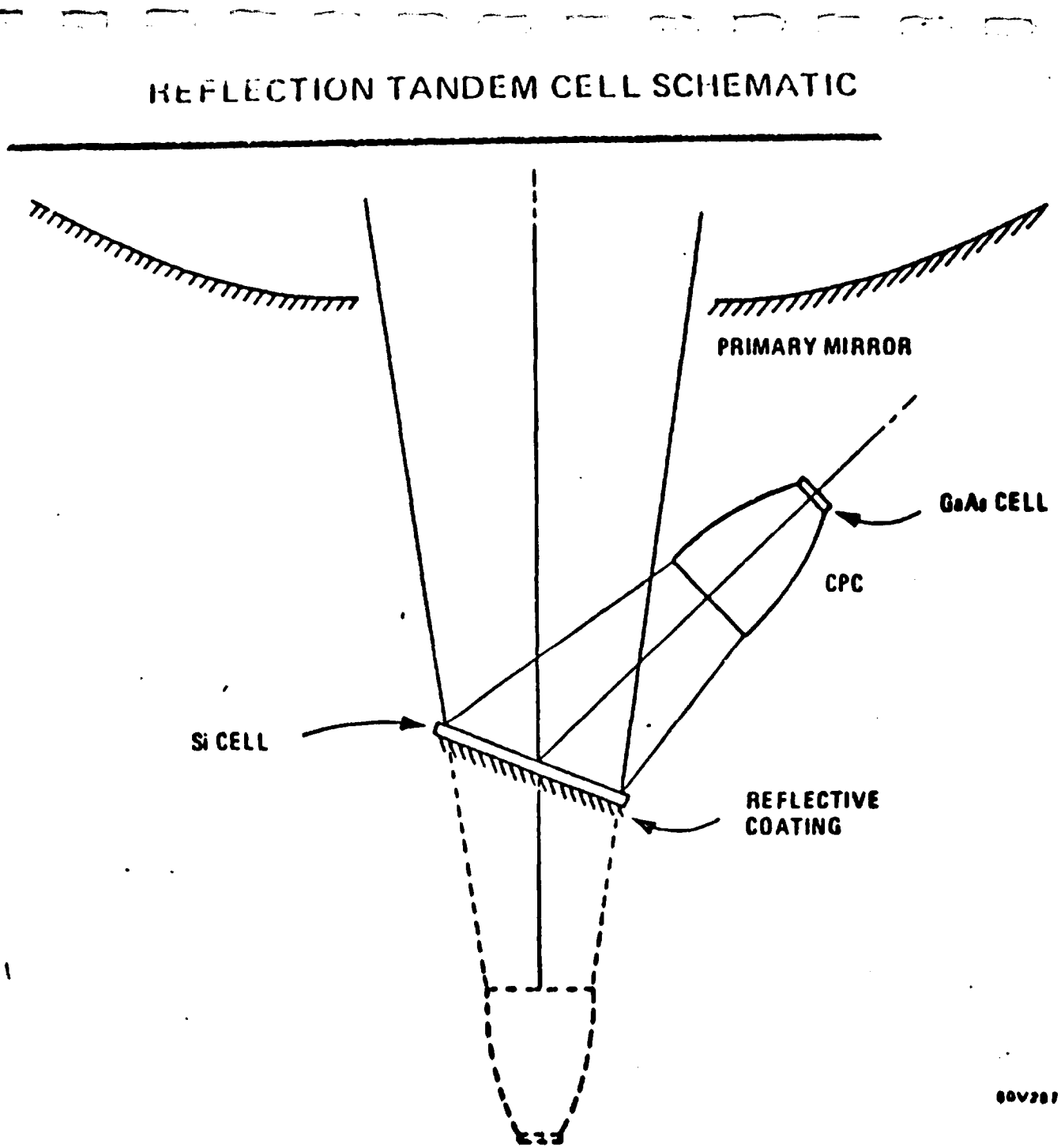

Figure 12. Tandem Cell Concept

For our 10" model, the dimensions of the GaAs cell are a 1" minor axis by 1.13" major axis, if oriented at 22^{o} from the optical axis. This results in an effective concentration ratio at the GaAs cell of 90, while the CR at the GaAs cell could be either 270 (without CPC) or 1000 (with CPC). This concept also works with Si and GaAs cells interchanged. It would be a relatively easy matter to test both the nominal 2-cell model and a reflective tandem 2-cell arrangement, since most of the model configuration remains unchanged. We plan to investigate this concept further, along with the availability of the larger Si solar cell.

2.4 Beamsplitter Design

Design Concept

The air mass zero or extraterrestrial solar spectrum covers from 0.2 μm to about 4.0 μm, with ∿ 75% of the energy contained between 0.2 μm to 1.1 μm. The energy between 0.2 μm to 0.3 μm is about 1%.

In this program, the beamsplitters to be designed are those for the two-cell GaAs/Si and Si/GaAs configurations, i.e., both reflection and transmission modes to the GaAs cell will be designed. The beamsplitter for the GaAs/Si configuration reflects 0.3 to 0.9 μm to GaAs while transmitting the longer wavelengths to Si as shown in Figure 13. However, only the 0.9 to 1.1 μm portion of the spectrum is utilized by the Si cell. The beamsplitter for the Si/GaAs configuration reflects 0.9 to 1.1 μm to the Si cell while transmitting the short wavelengths to GaAs as shown in Figure 14.

The beamsplitters designed to date in this program were based on the spectral quantum efficiency calculated in Phase I program, which showed no cut-off in short wavelengths for both GaAs and Si cells. A practical consideration is to use the spectral quantum efficiency cut-off of the state-of-the-art R&D cells. The GaAs and Si cells cut-off at short wavelengths is somewhere between 0.4 - 0.5 μm. More detailed information is being collected from several R&D laboratories. The final modification of the beamsplitter designs will be made according to the spectral quantum efficiency curves of the state-of-the-art cells.

Material Selection

The beamsplitter coatings consist of multilayer stacks of transparent dielectric materials. By depositing alternating high and low refractive index dielectric layers on a substrate, very high reflectivity can be achieved over a well-defined spectral range. The spectral width of the reflection band

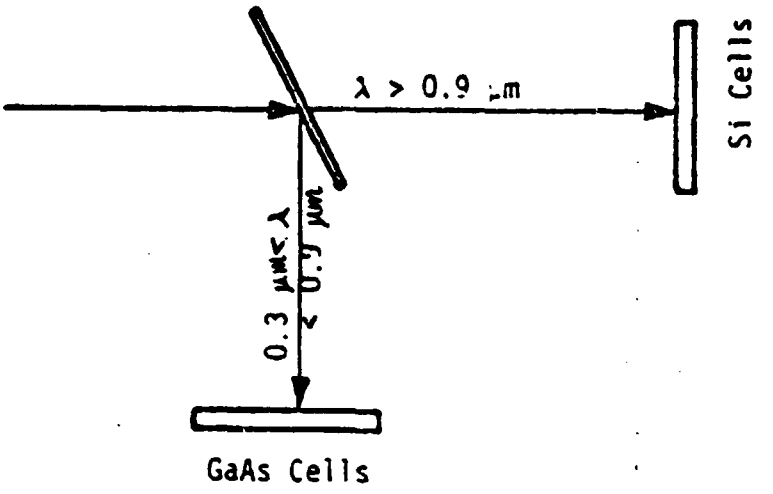

Figure 13. Spectrum Splitting Concept For Two-Cell GaAs/Si Configuration

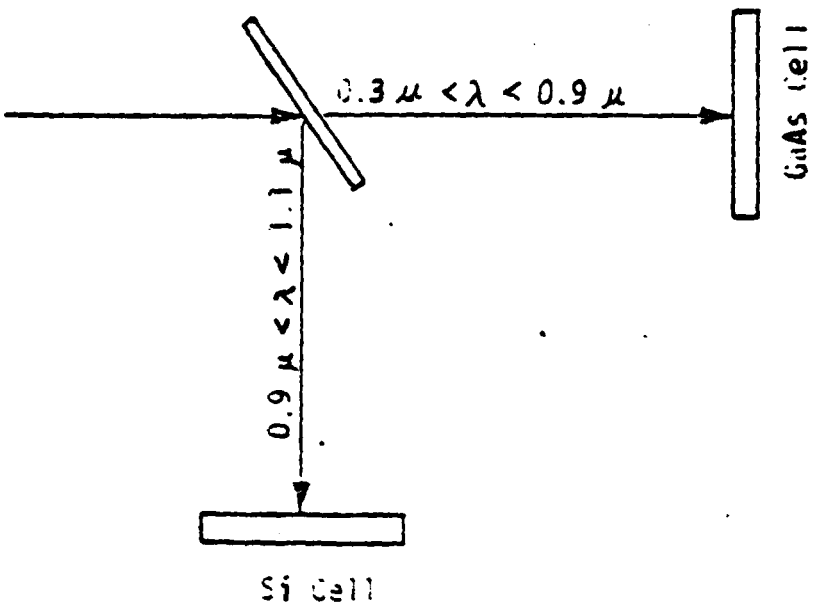

Figure 14. Spectrum-Splitting Concept for Two-Cell Si/GaAs Configuration

increases with the increase of the ratio of refractive indices used in the stack. Therefore, for the wide reflection spectral range (0.3 - 0.9 μm), one of the important material selection criteria is the high ratio of refractive indices of the material. UV transparency is also a primary concern. A list of the candidate materials is given in Table 2.

The Ta_2O_5/MgF_2 combination is selected for the beamsplitter for the GaAs/Si configuration instead of ThO_2/MgF_2 (which was used in the Phase I program) because Ta_2O_5/MgF_2 has a higher ratio of refractive indices. This makes the total number of layers required for the beamsplitter to be 65 layers, or three stacks instead of 86 layers or four stacks of ThO_2/MgF_2. The larger the number of stacks, the more potential fabrication and durability problems are anticipated. The larger number of stacks also tends to have higher off-band reflection ripples in the 0.9 - 1.1 μm region which are undesirable.

A combination of CaF_2/ThO_2 is selected for the beamsplitter for the Si/GaAs configuration. ThO_2 is chosen instead of SiO_2 in Phase I since the transmission range of SiO_2 starts at 0.35 μm and renders it unsuitable for a single beamsplitter system.

Beamsplitter Design

The design details of the beamsplitter with a combination of Ta_2O_5/MgF_2 coatings on a quartz substrate are given in Figure 15. The spectral reflectance of the beamsplitter at incident angles of 0 and 22.5 degrees are shown in Figures 16 and 17, respectively.

The reflection loss from 0.9 to 1.1 μm which cannot be utilized by either the Si or GaAs cell, is about 5%. The AMO solar energy from 0.2 to 0.3 μm is only about 1%. The Ta_2O_5/MgF_2 beamsplitter design reflects an average of more than 60% in this region. This would degrade the input to GaAs cell by 0.6% of the total spectral energy. Adding another stack to the coating could extend 100% reflection to 0.2 μm, but the trade-offs would be less durability and greater difficulty of fabrication.

TABLE 2. KEY PROPERTIES OF CANDIDATE COATING MATERIALS

	MATERIAL	TRANSMISSION RANGE (μm)	REFRACTIVE INDEX		STRESS ** (Kg/cm^2)	THERMAL EXPANSION COEFFICIENT (10^{-6}/°C)	MELTING POINT (°C)	SOLUBILITY * IN WATER (g/100 ml)	
			λ (μm)	n				COLD	HOT
HIGH REFRACTIVE INDEXES	ThO_2	0.21–(>5.0)	<1	2.20	950 (T)	9.5	3050	i	i
	Y_2O_3	0.22–(>5.0)	0.4 1.0	1.92 1.83	—	6.7 (20°C)	2410	0.00018	–
	Ta_2O_5	0.27–(>5.0)	< 1	2.42	—	–	1800	i	i
	ZrO_2	0.3 –7.0	0.55	2.1	—	7.5 (68–600°F)	2700	i	i
	TiO_2	0.43–6.0	0.6 0.8	2.29 2.21	200(T), 1000(C)	9.2 (40°C)	1830	i	i
	ZnSe	0.5 –2.0	0.6328 1.1	2.60 2.45	1200 (C)	7.7	>1100	i	–
	ZnS	0.35–14.5	0.578 1.529	2.36 2.28	2000 (C)	6.3 (0°C)	1820	0.000065	–
LOW REFRACTIVE INDEXES	MgF_2	0.11–7.5	0.40 1.00	1.40 1.38	2000 (T)	11.8	1266	0.0076	i
	SrF_2	0.25–15	0.546 1.129	1.48 1.47	1200 (T)	18.4	1280	0.1225	sl.s
	SiO_2	0.35–4.5	0.6328 1.13	1.42 1.46	2000 (C)	0.5	1610	i	i
	CaF_2	0.13–12	0.5 1.0	1.44 1.43	100 (T)	22.0	1360	0.0016	0.0017

* i — insoluble
sl.s — slightly soluble

** T — tensile stress
C — compressive stress

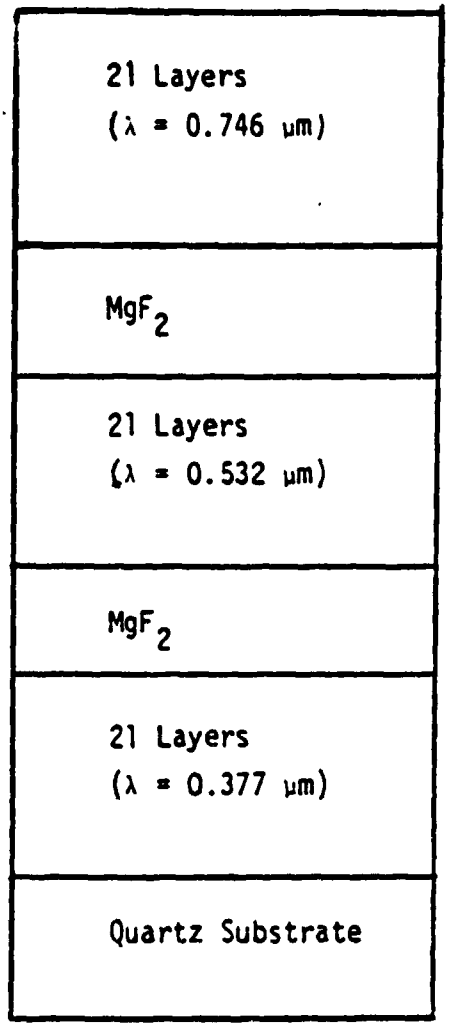

$n_H = 2.42$, $n_L = 1.38$

Layers 45 and 65: $t = \lambda/8n_N = 0.39$ μm
Layers 47, 49,...65: $t = \lambda/4n_H = 0.77$ μm
Layers 46, 48,...64: $t = \lambda/4n_L = 0.135$ μm

Layer 44: $t = 0.116$ μm

Layers 23 & 43: $t = \lambda/8n_H = 0.028$ μm
Layers 25, 27,...,41: $t = \lambda/4n_H = 0.055$ μm
Layers 24, 26...,42: $t = \lambda/4n_L = 0.096$ μm

Layer 22: $t = 0.082$ μm

Layers 1 & 21: $t = \lambda/8n_H = 0.019$ μm
Layers 3, 5,...,19: $t = \lambda/4n_H = 0.039$ μm
Layers 2, 4,...,20: $t = \lambda/4n_L = 0.068$ μm

$n_s = 1{:}46$

Figure 15. Details of the 65-Layer Ta_2O_5/MgF_2 Beamsplitter Coating Design (t = Physical Thickness)

Figure 16. Computed Spectral Reflectance of a 0.3 to 0.9 μm Reflective Ta_2O_5/MgF_2 Beam Splitter (65-Layer)

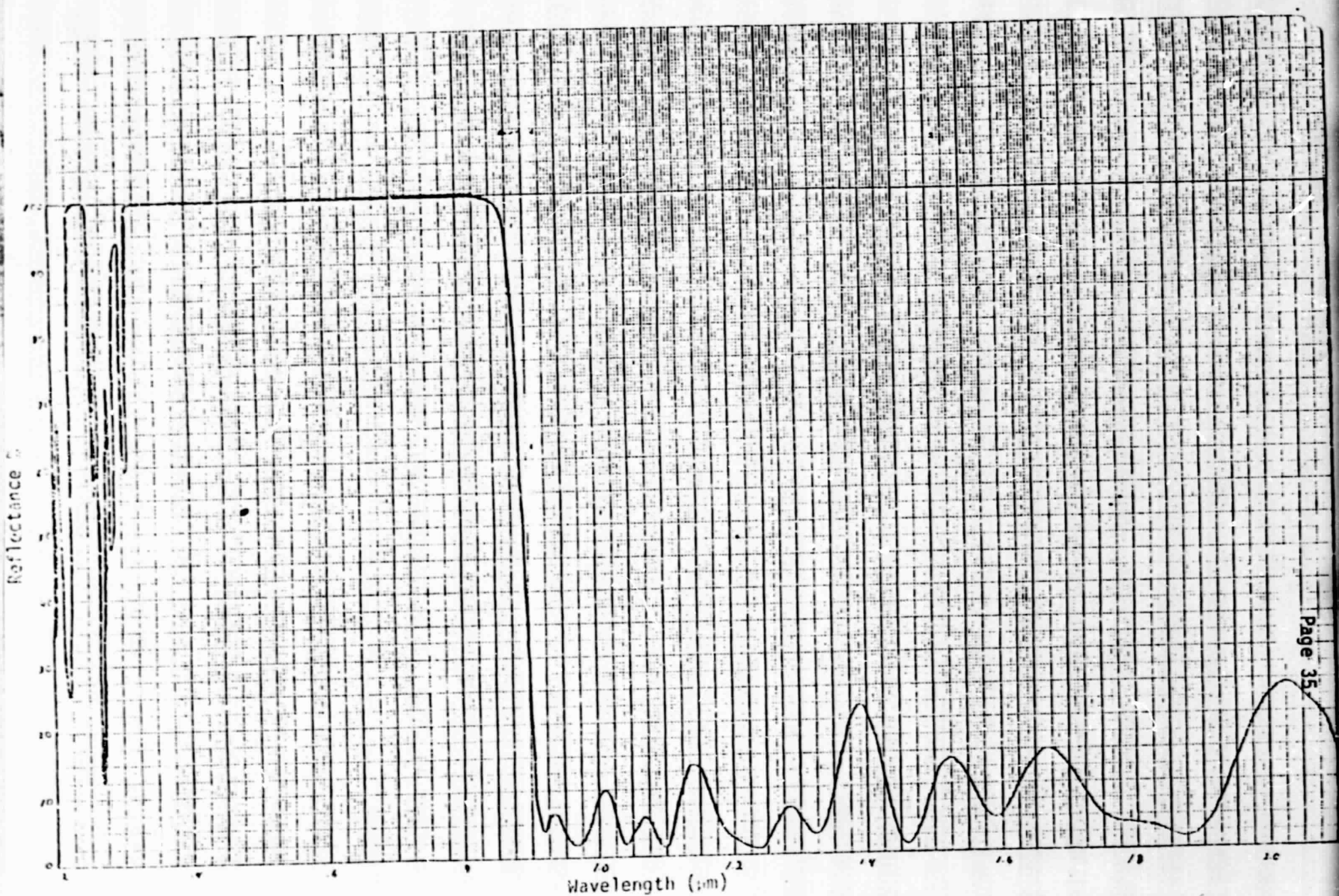

Figure 17. Computed Spectral Reflectance of a 0.3 to 0.9 μm Reflective Ta_2O_5/MgF_2 Beamsplitter (65-Layer Triple Stack, $\theta = 22.5^\circ$)

A tradeoff is conceivable that relaxes the requirements of the ideal beamsplitter, i.e., the sharp cut-on/cut-off at 0.9 μm, since Si cells can also convert the shorter wavelength radiation into electricity only at a lower efficiency than GaAs. The advantage of relaxing the beamsplitter design is in reducing the number of eielectric layers required, thus enhancing the yield and durability of the beamsplitter.

The details of the beamsplitter design for the Si/GaAs configuration are given in Figure 18. The predicted spectral reflectance of a 21-layer CaF_2/ThO_2 is shown in Figure 19. The reflection ripples beyond 1.1 μm would not be utilized by the system and therefore are of no concern. However, the reflection losses at wavelengths shorter than 0.9 μm have to be reduced.

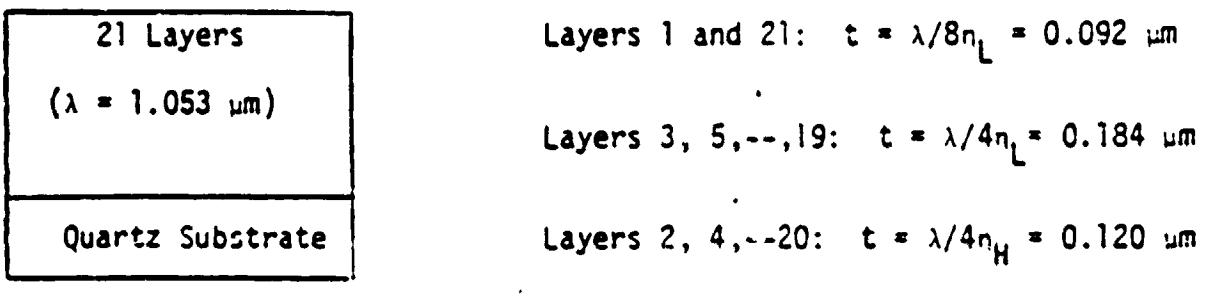

Figure 18. Details of the 21-Layer CaF_2/ThO_2 Beamsplitter Coating Design (t = Physical Thickness)

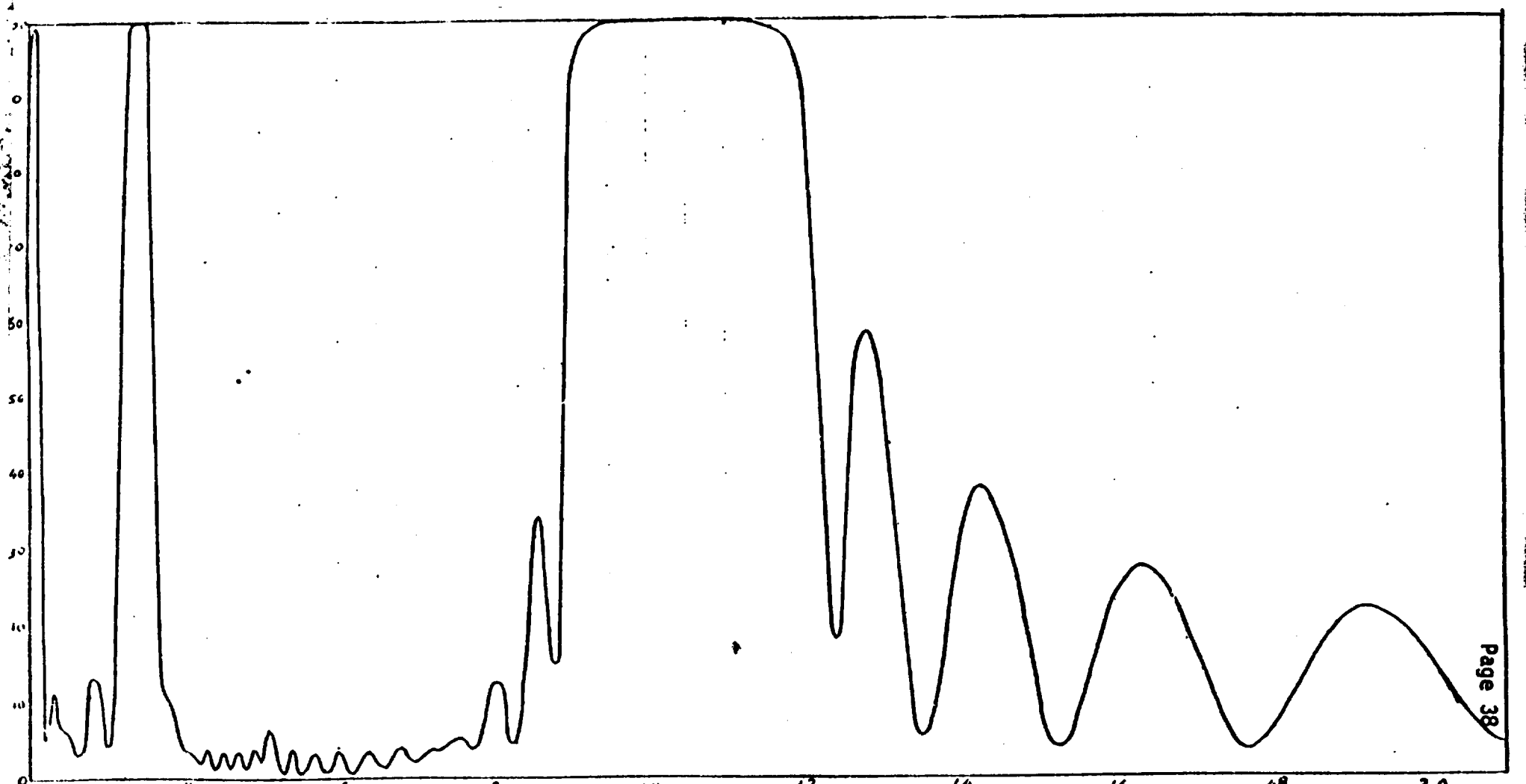

Figure 19. Computed Spectral Reflectance of a 0.9 - 1.1 μm Reflective CaF_2/ThO_2 Beam Splitter (21 Layers, $\theta = 22.5^{o}$)

2.5 Thermal/Mechanical Design

Spectral energy distribution and solar cell conversion efficiencies have been calculated for the two beamsplitter and solar cell configurations. These results are shown in Figure 20.

The convention adopted for calculating energy conversion efficiency for the spectrophotovoltaic concentrator system was to base the efficiency on the total flux intercepted by the primary mirror including the central obscuration. This results in conversion efficiencies which are lower than expected if compared to single cell performance, but more realistically includes concentrator optical losses.

The cutoff wavelength for GaAs is 0.9 microns. Shorter wavelengths are directed to the GaAs cell, while longer wavelengths are directed to the Si solar cell. The spectral energy distribution tabulated was claulcated assuming a beamsplitter spectral reflectance of 99% and a 90% spectral transmission. The remaining energy being absorbed in the beamsplitter coatings or scattered out of the concentrated beam.

The conversion efficiency of the GaAs and Si cells are calculated values using the models and equations provided in the Phase I final report. Included in these calculations are all of the concentrator reflection losses (ρ = 0.95), beamsplitter losses, grid shadowing and antireflection coatings losses. The calculations indicate a system conversion efficiency of 23.6% for GaAs/Si and 20.9% for Si/GaAs configurations can be obtained.

Concentrating photovoltaic systems produce high thermal fluxes which must be accounted for in the system design. Figure 21 tabulates the heat absorption associated with each of the major components in concentrator system. The primary mirror has a concentration of unity and therefore requires no cooling. The secondary mirror sees a concentration of approximately 10 : 1 but its absorptance is only 5%. By increasing its long wave length emittance

			GaAs/Si	Si/GaAs
% Spectral Energy To	GaAs		66.9%	78.7%
	Si		28.2%	11.2%
Conversion Efficiency of	GaAs		21.3%	18.3%
	Si		2.3%	2.6%
		TOTAL	23.6%	20.9%

Assumes 99% Reflection and 90% Transmission at Beamsplitter

Figure 20. Spectral Energy Distribution and Solar Cell Conversion Efficiency

Power At Beamsplitter	32.8W
Power Density	8.0 W/cm^2

Thermal Energy Absorbed	GaAs/Si Configuration	Si/GaAs Configuration
GaAs Cell	5.90 W	5.09 W
CPC	1.42 W	1.83 W
Si Cell	0.10 W	0.11 W
CPC	0.85 W	0.30 W
	8.27 W	8.33 W

Figure 21. Component Thermal Rejection Requirements

with selective coatings or blackening the back side and shading it from direct sun light its temperature can be controlled.

The absorption at the beamsplitter directly affects its equilibrium temperature. If the absorptance is 1% and the long wave emittance is 0.5 for each surface, the equilibrium temperature would reach 390K. A 2% absorptance coating would result in a 440 K beamsplitter temperature. During terrestrial testing, convection will limit the temperature rise to very small amount.

Thermal energy absorbed by the solar cells and CPC's requires auxiliary cooling and is of sufficient magnitude to be measured. The heat fluxes are tabulated in Figure 21 for the two configurations. The results show that cooling of the GaAs cell is far more critical than any other component in the system.

The measurement of CPC and solar cell temperature and heat flux will be performed using the insulated support shown in Figure 22. The CPC and solar cell will be supported in a metal jacketed, polyurethane foam insulated box. Cooling will be provided by conduction through 1/4 diameter copper rods attached to a water cooled heat sink. Heat flux will be inferred from the measured temperature gradient in the cooling rods.

The table included in Figure 23 provides the conductivity data, the sensitivity and an estimate of the heat loss through the insulation. A major uncertainty will be the amount of convective cooling that will occur. This effect can be minimized by operating the system with the CPC and solar cell temperature at or slightly below ambient air temperature.

The primary objective of the test program will be the evaluation of solar cell performance under high concentration spectrally selected fluxes. The terrestrial solar spectrum varies widely in both spectral distribution and total energy content. These variations are the result of atmospheric attenuation which can vary randomly due to local and wide spread water vapor,

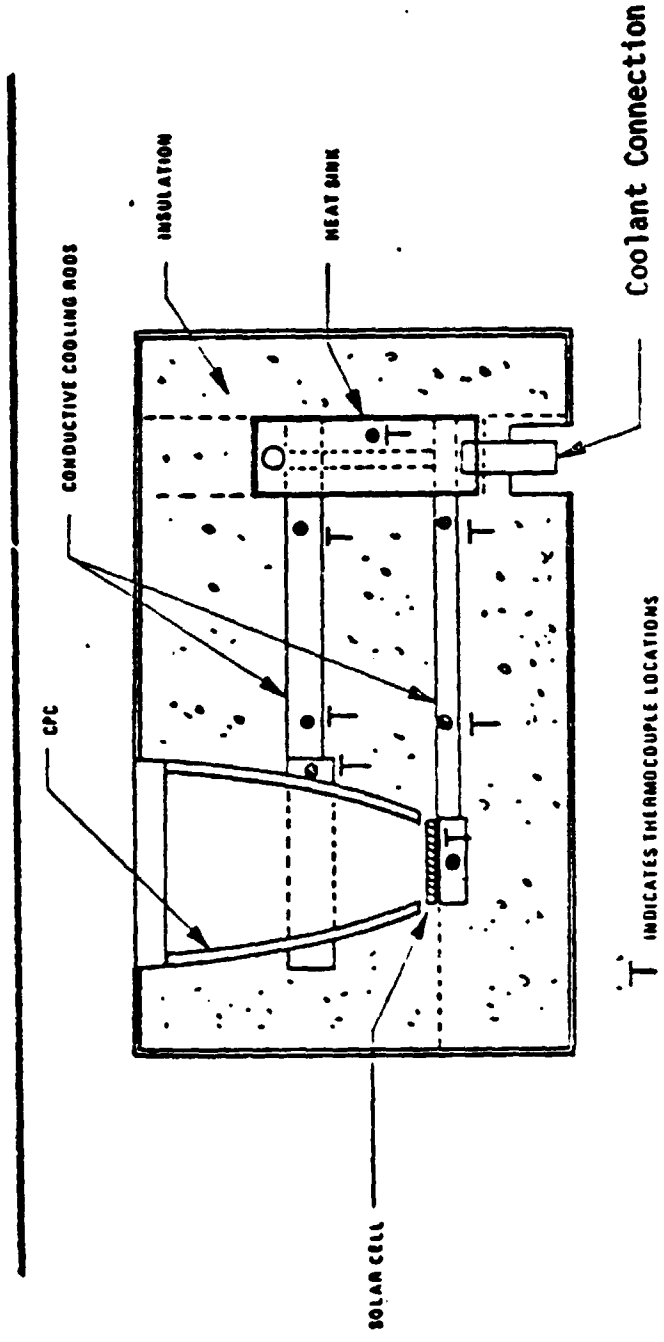

Figure 22. Thermal Measurements Sensitivity

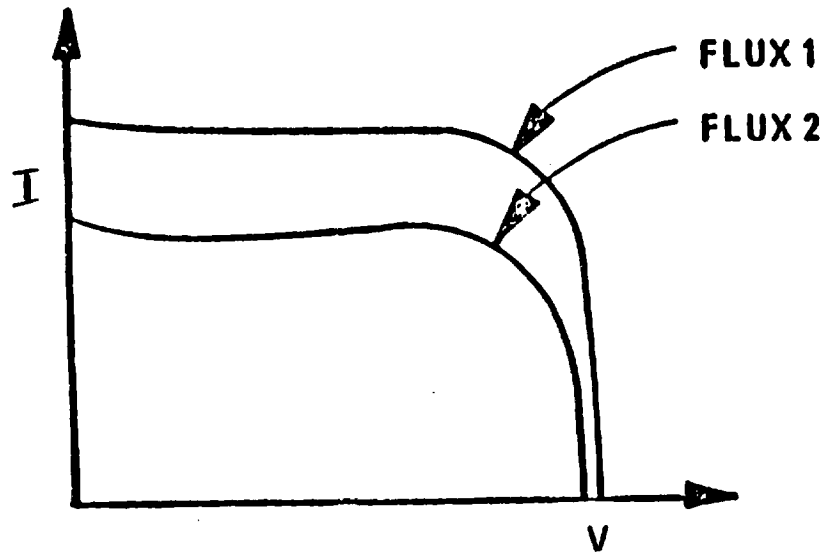

SOLAR FLUX MEASUREMENTS

STANDARD SILICON SOLAR CELL

PYRHELIOMETER

- **CLEAR APERTURE**
- **STANDARD SCHOTT GLASS SPECTRAL FILTERS**

Figure 23. Electrical Power Measurements

CO_2 and aerosol content, together with changes in solar evaluation angle. Terrestrial solar cell testing will require careful calibration of comparison stnadards. Simultaneous measurement of solar cell output and the solar direct and spectral energy content are required to obtain correlatable test results.

Figure 23 illustrates the typical type of current-voltage (I-V) curve that can be expected from a solar cell. Drawing the I-V curve allows determination of the maximum power point for each flux level. The instrumentation required to obtain these curves consists of an X-Y recorder and a variable resistor. The input to the recorder is obtained from cell voltage and current measurements. The curve is traced out by varying a cell series resistor from 0 to infinity.

Solar total flux measurements can be obtained with a calibrated pyrheliometer. Additionally, the spectral energy distribution can be obtained using spectral filters in conjunction with the pyrheliometer. Another aid in determining spectral energy content is to use a standard solar cell whose current output has been characterized as a function of illumination level by one of the government laboratories such as NASA Lewis Research Center.

The I-V characteristics together with the solar flux measurements will characterize the solar cell. These measurements will permit extrapolation of the test results to different intensity levels and to different spectral energy distribution conditions.

The subscale test model can easily be accommodated by an amateur telescope mount. The weight of the telescope may be slightly greater than most mounts are designed to accommodate, but the compact design has a very low radius of gyration. This coupled with the low tracking precision requirements compared with astronomical measurements, makes an amateur telescope mount drive an ideal support system. Figure 24 is a scale drawing of the subscale test model mounted on a pedestal mount with a clock motor drive system.

TELESCOPE DRIVE AND SUPPORT

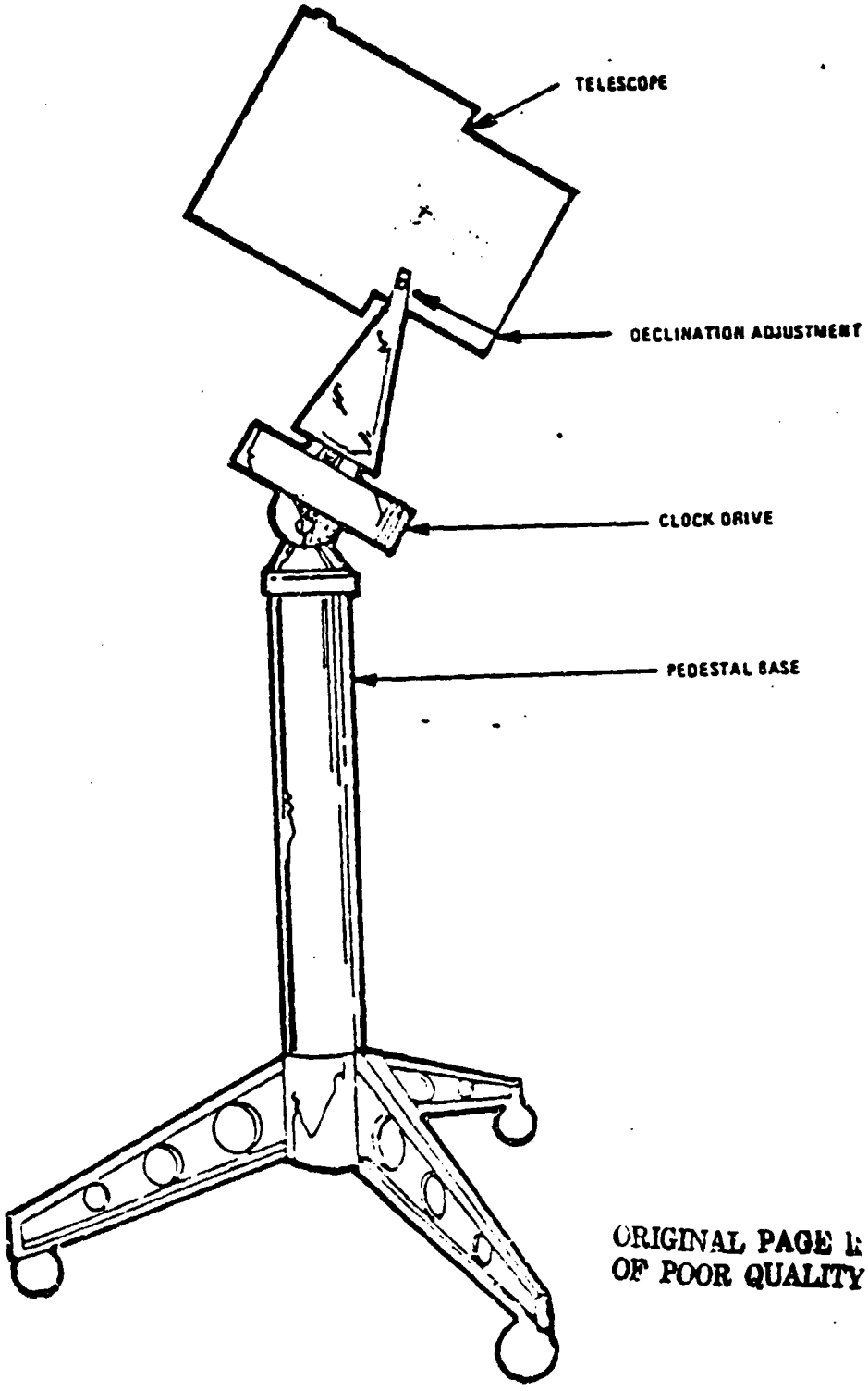

Figure 24. Telescope Drive and Support

2.6 Model Costing

The cost of the model is based on the following task breakdown:

1. Procure/Fabricate Components

   - Mount (10" fork with drive)
   - Primary + secondary mirrors
   - CPC's
   - Telescope body/mounting
   - Beamsplitters (2 designs)
   - Solar cells

2. Component Testing

   - Surface profile + reflectance measurements
   - System thruput measurements
   - Calibration
   - Solar cell thermal tests
   - Solar cell electrical tests
   - Beamsplitter

3. System Integration

   - Mount components
   - Electronics
   - Optical alignment
   - Analytic performance predictions

4. System Laboratory Testing

- Test equipment calibration
- Lab tests
- Data analysis
- Test report

5. System Field Testing

- Site preparation
- Test set-up
- Testing
- Data analysis
- Report

6. Lab Simulator Modification

- Hardware design changes
- Hardware costs
- 10" collimator optics
- Xenon lamps
- Testing/calibration

7. Reporting

- Final reports
- Management/Financial Reports

Tasks 1-3 are model building and Tasks 4-6 are model testing. The estimated cost for building the model is ∿ $160K and for testing it is ∿ $50K.

The suppliers for the components have been identified and are listed in Table 3.

TABLE 3. SUPPLIERS FOR MODEL COMPONENTS

COMPONENTS	SUPPLIERS
OPTICS	
PRIMARY	HEOC (DIAMOND TURNED)/
SECONDARY	SPECIAL OPTIONS CO. (CONVENTIONAL)
BEAMSPLITTER	IN HOUSE
CPC	OPTICAL RADIATIONS CORP.
MECHANICAL/THERMAL	
TELESCOPE SUPPORT STRUCTURE	IN HOUSE
THERMAL MEASUREMENT	IN HOUSE
FIXTURES	
MOUNT AND TRACK STRUCTURE	EDMUND SCIENTIFIC
SOLAR CELL	
GaAs	• VARIAN • ROCKWELL INTERNATIONAL
Si	• SOLAREX • APPLIED SOLAR ENERGY
LONG LEAD ITEMS > 3 MONTHS	
	PRIMARY
	SECONDARY
	SOLAR CELLS

2.7 Testing Plan

Tests will be carried out to obtain information as given in Table 4.

2.8 Related Activities

As a conclusion to the first phase activity on this program, Joan Onffroy presented a paper "High-Efficiency Concentrator/Multi-Solar Cell System for Orbital Power Generation". This was presented on 19 August at the 15th Intersociety Energy Conversion Engineering Conference. This paper appeared to be well received by the audience.

Reports from the final presentations made for the study of Multi-KW Solar Arrays for Earth Orbit Applications were received from Rockwell International, Lockheed and TRW. These have been reviewed and a written summary of applicable sections was prepared for the current research team members. The mini-Cassegrain version suggests that an optimal design might consist of a number of smaller concentration modules. A single 1000 : 1 cohcentration system producing 50 - 100 kW of power should be compared to a system with many high concentration submodules. This comparison would identify the most viable approach in terms of cost effectiveness.

A mid-term oral review was presented at NASA Marshall on 8 December 1980. The review was favorable and complimentary to the team's accomplishments.

TABLE 4. TESTING PLAN

COMPONENTS	INFORMATION
OPTICAL, MIRRORS CPC	• REFLECTANCE, • SURFACE PROFILES • C.R. (EACH STAGE)
BEAMSPLITTER	• REFLECTION CHARACTERISTICS • THERMAL ENDURANCE (TEMP. CYCLING AND THERMAL SHOCKS) • UV RESISTANCE • TRANSMISSION
SOLAR CELLS	• SPECTRAL QUANTUM EFFICIENCY • I-V CHARACTERISTICS vs. INTENSITY • I-V CHARACTERISTICS vs. CELL TEMP.
THERMAL MONITOR	• CALIBRATION
INTEGRATED SYSTEM	• ELECTRICAL OUTPUT vs. INPUT FLUX (INTENSITY, SPECTRUM) • THERMAL OUTPUT vs. INPUT FLUX

3.0 PROGRAM MANAGEMENT

3.1 Program Financial Status

The design tasks are slightly behind schedule. Ahead of schedule are the model costing and testing plan.

The program spending and status is displayed in Table 5. All tasks should be completed by the end of January 1981. Two weeks are reserved for final reporting and an oral presentation scheduled on 15 February 1981.

TABLE 5.

PAGE 1 OF 2 PAGES

NATIONAL AERONAUTICS AND SPACE ADMINISTRATION
MONTHLY CONTRACTOR FINANCIAL MANAGEMENT REPORT

Form Approved
Budget Bureau No. 104-R0011

2. REPORT FOR MONTH ENDING AND NUMBER OF OPERATING DAYS: Date - 12/07; Operating Days - 18

TO: PROCUREMENT OFFICE
Geo. C. Marshall Space Flight Center
Nat'l Aero & Space Admin.
Marshall Space Flight Center, AL 35812
Doris M. Grubbs

FROM: HONEYWELL INC.
Systems and Research Center
2600 Ridgway Parkway PO 312
Minneapolis, MN 55440

1. DESCRIPTION OF CONTRACT
a. TYPE: CPFF
c. SCOPE OF WORK

b. CONTRACT NO. AND LATEST DEFINITIZED AMENDMENT NO: NAS8-33511 Agreement 4

d. AUTH. CONTR. REP. (Signature): J. Chaffin / S. Lo DATE: 12/10/80

3. CONTRACT VALUE
a. COSTS: $89,427
b. FEE: $ 6,669

4. FUND LIMITATION
$89,427 $ 6,669

5. BILLING
a. INVOICE AMTS BILLED: $75,151
b. TOTAL PYTS RECD: $47,849

6. REPORTING CATEGORY	7. COSTS INCURRED HOURS WORKED — DURING MONTH ACTUAL a.	DURING MONTH PLANNED b.	CUM. TO DATE ACTUAL c.	CUM. TO DATE PLANNED d.	8. ESTIMATED COSTS HRS. TO COMPLETE — DETAIL a.	DETAIL b.	BALANCE OF CONTRACT c.	9. ESTIMATED FINAL COSTS HOURS — CONTRACTOR ESTIMATE a.	CONTRACT VALUE b.	10. UNFILLED ORDERS OUTSTANDING
Phase I TASKS										
F0719-AA-0001-2882 Solar Cells	0		9,499							11,429
F0719-BB-0001-2882 Beam Splitter	0		11,080							11,249
F0719-CC-0001-2882 Systems Performance	0		9,601							9,655
F0719-DD-0001-2882 Program Management	9		7,727							5,829
Phase II										
F0719-EE-0001-2886 Model Def.	0		5,102							5,103
F0719-FF-0001-2886 Optics Design	2,355		4,828							7,948
F0719-GG-0001-2886 Beam Splitter Design	938		6,500							6,802
F0719-HH-0001-2886 Mech/Thermal Design	2,065		3,765							5,603
F0719-JJ-0001-2886 Testing Plan	0		0							4,812
F0719-KK-0001-2886 Model Costing	0		0							1,777
F0719-MM-0001-2886 Mgmt.-Reporting Admin.	1,266		2,873							4,983
Total LBM	6,633		60,975							75,190
G&A Rates 1979 = 17.3% 1980 = 17.0%	1,129		10,451							13,121
Cost	7,762		71,426							88,311
COM .01264	99		903							1,116
Fee .07552	586		5,394							6,669
Price	8,447		77,723							96,096

Baseline Plan Identification (Col. 7b & 7d): Revision No. _____, Dated _____

NASA FORM 533M SEP 71 REPLACES NASA FORMS 533a, b AND c WHICH ARE OBSOLETE.

PHASE II PROGRAM STATUS CHART

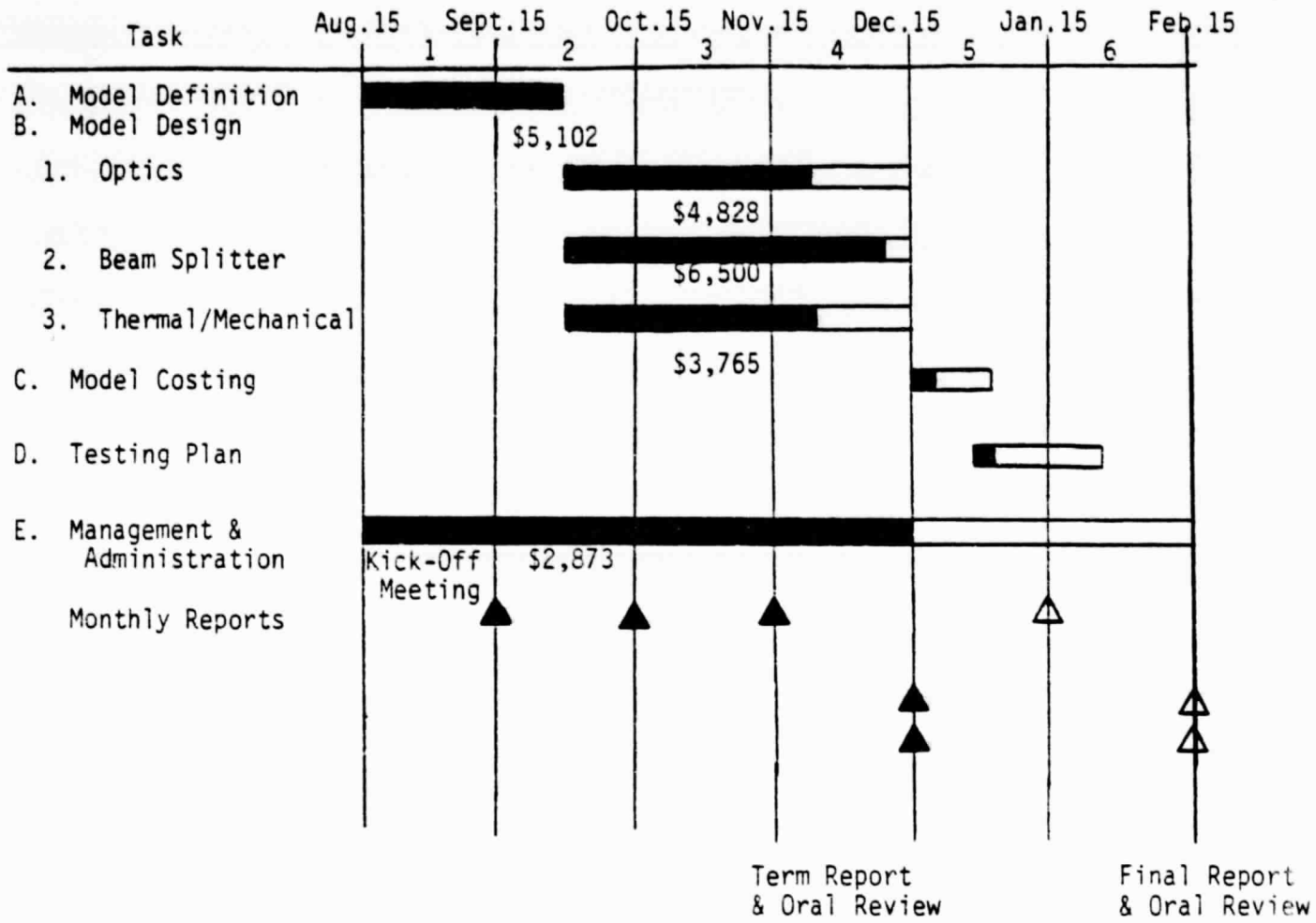

Work Scheduled

Estimated Work Completion

$ LBM$ Spent